Conducting and magnetic composites polypyrrole nanotubes/magnetite nanoparticles: Application in magnetorheology

Conducting and Magnetic Composites Polypyrrole Nanotubes/ Magnetite Nanoparticles: Application in Magnetorheology

Jaroslav Stejskal,* Irina Sapurina, Jarmila Vilčáková, Tomáš Plachý, Michal Sedlačík, Constantin Bubulinca, Marek Goralík, Miroslava Trchová, Zdeňka Kolská, and Jan Prokeš

Irina Sapurina — Centre of Polymer Systems, Tomas Bata University in Zlin, 760 01 Zlin, Czech Republic; Institute of Macromolecular Compounds, Russian Academy of Sciences, St. Petersburg 199004, Russian Federation

Jarmila Vilčáková — Centre of Polymer Systems, Tomas Bata University in Zlin, 760 01 Zlin, Czech Republic

Tomáš Plachý — Centre of Polymer Systems, Tomas Bata University in Zlin, 760 01 Zlin, Czech Republic

Michal Sedlačík — Centre of Polymer Systems, Tomas Bata University in Zlin, 760 01 Zlin, Czech Republic; @ orcid.org/0000-0003-3918-5084

Constantin Bubulinca — Centre of Polymer Systems, Tomas Bata University in Zlin, 760 01 Zlin, Czech Republic

Marek Goralík — Centre of Polymer Systems, Tomas Bata University in Zlin, 760 01 Zlin, Czech Republic

Miroslava Trchová — University of Chemistry and Technology Prague, 166 28 Prague 6, Czech Republic; © orcid.org/ 0000-0001-6105-7578

Zdeňka Kolská — Faculty of Science, J.E. Purkyně University, 400 96 Ústí nad Labem, Czech Republic Jan Prokeš — Faculty of Mathematics and Physics, Charles University, 180 00 Prague 8, Czech Republic Complete contact information is available at: https://pubs.acs.org/10.1021/acsanm.1c00063

Corresponding Author Jaroslav Stejskal − Institute of Macromolecular Chemistry, Academy of Sciences of the Czech Republic, 162 06 Prague 6, Czech Republic; orcid.org/0000-0001-9350-9647; Email: stejskal@imc.cas.cz

ABSTRACT:

The study aims at the design of nanostructured hybrid materials that are both conducting and magnetic. Conducting polypyrrole nanotubes were prepared by the oxidation of pyrrole with iron(III) chloride stimulated by the organic dye, methyl orange. The excess of oxidant involved in the synthesis was used for the in situ generation of magnetite nanoparticles after addition of ammonia that coated the polypyrrole nanotubes. The resulting composites of varying composition were characterized with respect to the specific surface area and by X-ray diffraction and FTIR spectroscopy. The conductivity measurements revealed that polypyrrole nanotubes had a conductivity of ≈20 S cm^{-1} and the composites with magnetite nanoparticles ≈1 S cm^{-1} virtually independent of the composition. While polypyrrole nanotubes had marginal magnetic properties, the saturation magnetization of composites reached ≈50 emu g^{-1}, close to that of neat magnetite. The reprotonation of polypyrrole in composites increased the conductivity to ≈5 S cm^{-1} at the expense of reduction of magnetic properties. The magnetorheological analysis was performed to illustrate their possible application exploiting the nanotubular morphology and requiring a magnetic response.

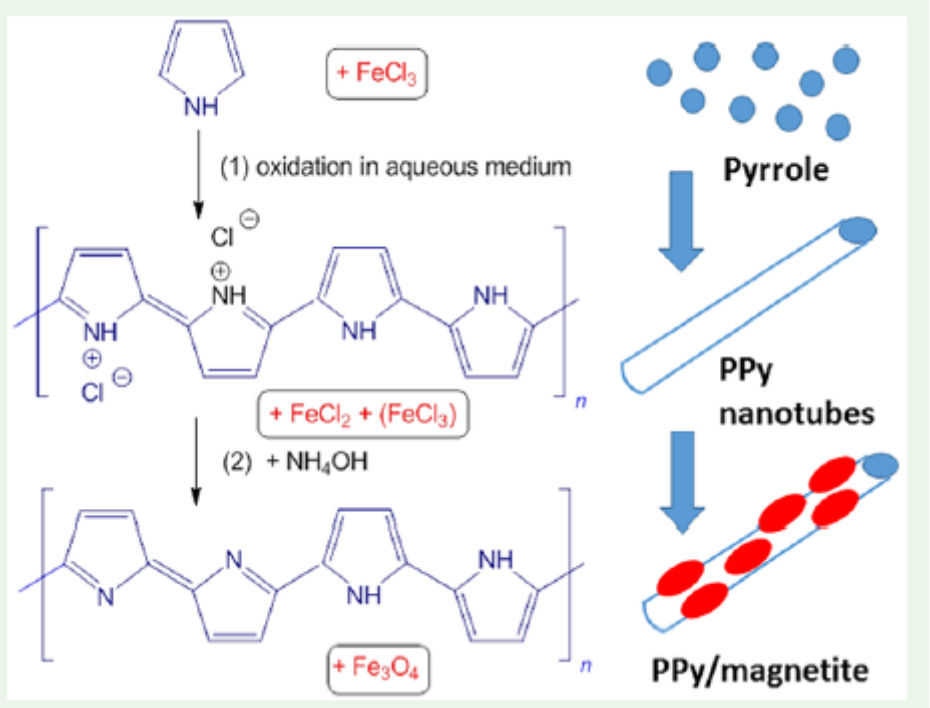

KEYWORDS: Conducting polymer, conductivity, polypyrrole nanotubes, magnetite, magnetic properties, magnetorheology

1. INTRODUCTION

Polypyrrole (PPy) is one of the most investigated conducting polymers due to the ease of preparation, conductivity at the semiconductor level, good environmental stability, and strong application potential.[1] It is obtained by the oxidation of pyrrole typically with iron(III) chloride in characteristic globular form.[2,3]

When the same preparation proceeds in the presence of suitable organic dyes,4 most often methyl orange, polypyrrole nanotubes are obtained instead.[4-6] They represent a superior organic conducting material applicable in various directions.6 The nanotubular morphology is uniform, and the conductivity is enhanced by 1 or 2 orders of magnitude up to 100 S cm^{-1} compared with a common globular form.[3,5,7] Nanotubes display also improved stability with respect to the loss of conductivity due to deprotonation under physiological conditions.[8,9] This makes them an organic conducting material of choice in the biomedical field.[1,10]

Polypyrrole nanotubes have been modified in various manners. For example' they have been coated with another conducting polymer' polyaniline,[11] to obtain new core-shell nanostructures. The introduction of surfactants to the synthesis also affected their properties.[12,13] Polypyrrole nanotubes have been most often decorated with various inorganic species providing a value-added upgrade' such as cobalt ferrite[14] layered double hydroxides,[15] manganese dioxide,[16,17] molybdenum disulfide,[18] nickel(ll) hydroxide,[19] tin(IV) oxide,[20-24] and noble-metal nanoparticles.[25-28] The composites of polypyrrole nanotubes with a magnetic component' magnetite (Fe_3O_4)' are newly described in this study.

The preparation of common polypyrrole/magnetite composite proceeds as a rule in two steps. Magnetite is prepared at first' and subsequently it is used as a substrate for the deposition of polypyrrole by in situ polymerization of pyrrole with iron(III) chloride. Note that both steps employ iron compounds as reactants. The coprecipitation approach using iron(ll) and iron(lll) chloride at 1:2 mole ratio in ammonia solution is probably the most common way to prepare magnetite particles.[29-32] Alternatively' they were produced by a solvothermal process involving the reduction of iron salts with ethylene glycol at elevated temperature.[33] Magnetite was then coated during in situ polymerization of pyrrole with iron(III) chloride as oxidant.[31-33] Commercial magnetite nanoparticles have also been used in the experiments.[34] Polypyrrole was also deposited by galvanostatic electrolysis resulting in polypyrrole-coated Fe_3O_4 core-shell colloids[34] (Fe_3O_4@PPy). All above syntheses yield composites with a magnetite core and polypyrrole shell.

Both steps can be reversed. For example, polypyrrole was prepared by the oxidation of pyrrole with iron(II) chloride along with hydrogen peroxide. The peroxide converted iron(II) chloride to iron(III) chloride, which subsequently oxidized pyrrole to polypyrrole. The fact that iron(III) chloride would be reduced back to iron(II) chloride at the same time, however, was not discussed. If the system used for the preparation of polypyrrole contained both the iron(II) and iron(III) ions, the addition of ammonia would produce magnetite in the next step.[35] Polypyrrole decorated or coated with magnetite is a result of such syntheses.

Polypyrrole/magnetite composites have been used in supercapacitor electrodes with enhanced specific capacity[36] and in photothermal therapy due to their ability to convert absorbed infrared irradiation to heat.[31] They were similarly tested for the electromagnetic radiation shielding.[32,35] The design of water-pollutant adsorbents separable by a magnetic field is another prospective application proposed in the literature.[33] The unique structure of polypyrrole/magnetite composite particles could be, besides the above-mentioned applications, used with benefits also in various systems responsive to a magnetic field. Magnetorheological fluids are one of the intelligent systems consisting of magnetic particles dispersed in a nonmagnetic carrier liquid. They can change their rheological properties in terms of continuous and reversible transition from a liquid-like viscous state to a solid-like elastic state in milliseconds by an applied external magnetic field.[37] The responsive character allows magnetorheological fluids to be used for diverse damping systems,[38] haptic devices,[39] polishing technology,[40] and so on.

The present study reports the one-pot preparation of polypyrrole nanotubes as a conducting core component that is coated with magnetite. The magnetorheological performance of such a nanostructured solid phase dispersed in liquid is demonstrated.

2. EXPERIMENTAL SECTION

2.1. Preparation

Reference polypyrrole nanotubes were prepared by the oxidation of pyrrole (0.7 mL, 10 mmol) with iron(III) oxide hexahydrate (6.76 g, 25 mmol) in 100 mL of water containing 65 mg of methyl orange at room temperature. The concentrations thus were 0.1 M pyrrole, 0.25 M iron(III) chloride, and 0.002 M methyl orange, the mole ratio [$FeCl_3$]/[pyrrole] = 2.5 being stoichiometric (**Scheme 1**). The presence of methyl orange ensures the generation of nanotubes instead of globular morphology.[6] All chemicals were purchased from Sigma-Aldrich and used as delivered. The first series of syntheses followed varying concentrations of iron(III) chloride from 0.25 to 0.6 M; that is, the oxidation was performed at a stoichiometric excess relative to pyrrole. The oxidant-to-monomer mole ratio [$FeCl_3$]/[pyrrole] = 2.5

— 6 was selected as a parameter to denote the individual samples. Polypyrrole nanotubes were isolated the next day by filtration, rinsed well with 0.1 M hydrochloric acid followed by acetone, and left to dry in open air.

The second series was prepared in the same manner, but instead of the isolation of the polypyrrole, pH was adjusted to 8—9 by 200 mL of 1 M ammonium hydroxide. This step converted residual iron(II)/ iron(III) salts to magnetite and related oxides and polypyrrole hydrochloride to a corresponding polypyrrole base8 (**Scheme 1**). The polypyrrole/magnetite solids were separated next day by filtration as above, rinsed with water until neutral reaction and then with acetone, and dried.

Scheme 1. (I) Pyrrole Is Oxidized with Iron(III) Chloride to Polypyrrole, and Iron(II) Chloride Is a Byproduct; (2) If Iron(III) Chloride Is Still Present, Magnetite Is Generated under Alkaline Conditions, and Polypyrrole Converts to a Base; and (3) Polypyrrole Base May Be Reprotonated to a Salt under Acidic Conditions

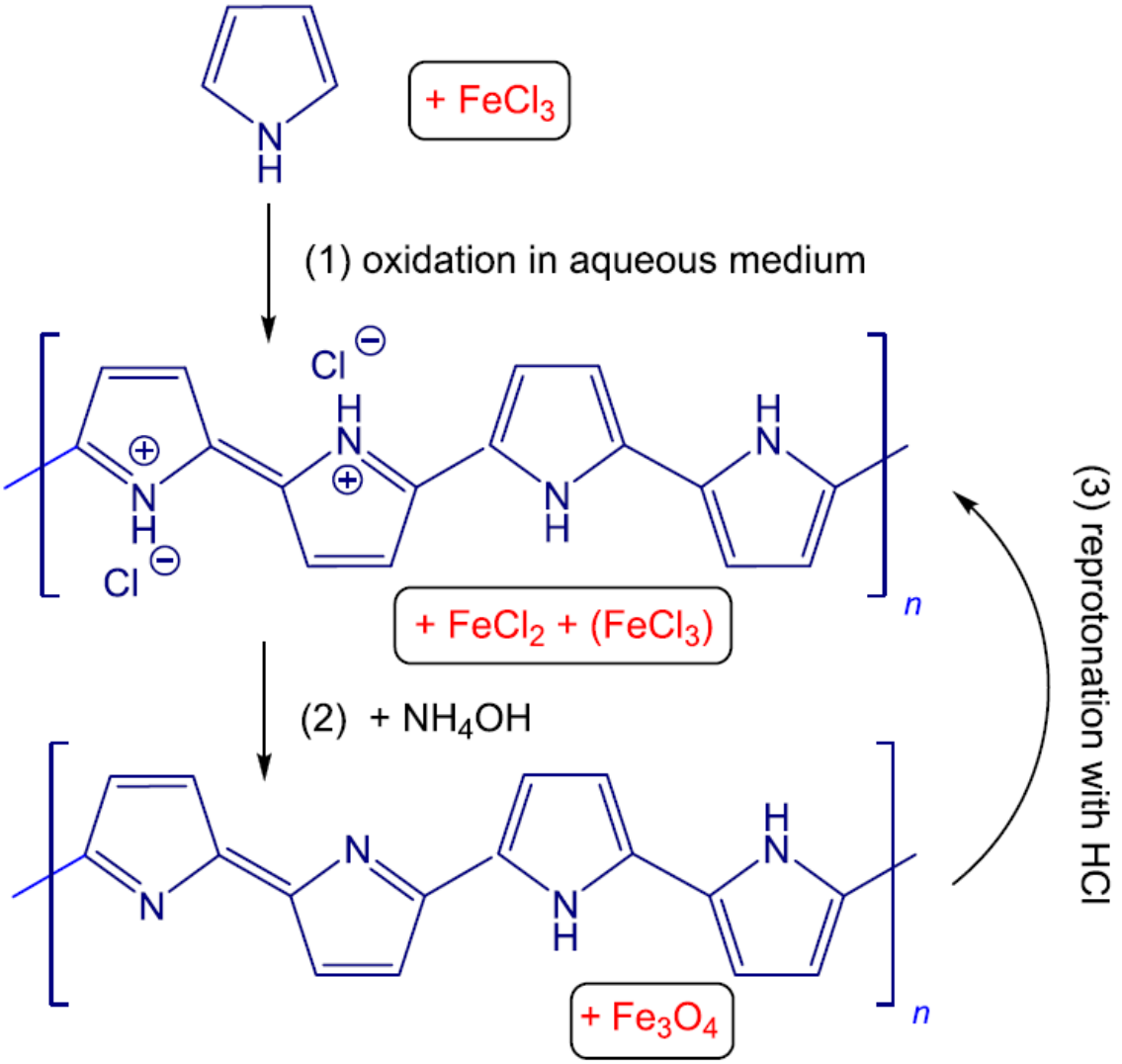

Finally, the third series followed the same protocol as the second, but the pH of the reaction mixture was converted to 1—2 by addition of hydrochloric acid before the product separation (**Scheme 1**). This step partly recovered the polypyrrole base to polypyrrole salt9 and dissolved some of the iron oxides. Finally, the solids were rinsed with 0.1 M hydrochloric acid and then acetone and dried.

2.2. Characterization

The morphology was observed with a FEI Tecnai T12 electron microscope FEI operated at 120 kV. The content of inorganic part represented by magnetite and/or other iron oxides was determined to be an ash. The specific surface area and pore volume were determined from adsorption/desorption isotherms with aNOVA3200 (Quantachrome Instruments) using NovaWin software. The structure of magnetite was confirmed with an X-ray diffractometer (Advance D8, Bruker) using Cu Ka radiation. FTIR spectra were analyzed by using a Nicolet 6700 (Thermo-Nicolet, USA) spectrometer equipped with a reflective ATR extension GladiATR (PIKE Technologies, USA) with a diamond crystal. The conductivity was determined by the four-point van der Pauw method on pellets 10 mm in diameter and ca. 1 mm thick prepared at 527 MPa in a hydraulic press when such a preparation was feasible. Magnetic characteristics of prepared nanocomposites were investigated by a vibrating sample magnetometer (VSM, Model 7407, USA).

2.3. Magnetorheology

The magnetorheological properties were examined for the system containing 15 wt % composite prepared at [$FeCl_3$]/[pyrrole] = 4 and 6 in silicone oil (Lukosiol M100, Chemical Works Kolin, Czech Republic; viscosity 100 mPa s, density 0.965 g cm^{-3}) by using a rotational rheometer (Physica MCR502, Anton Paar, Austria) equipped with a magneto-cell (MRD 180/1T) and parallel-plate geometry (PP20/MRD/TI/S) with a measuring gap of 0.3 mm. The suspensions were mechanically stirred, and the magnetic field was applied 1 min before starting the measurement. The value of external magnetic field strength applied was set to 61, 122, and 176 kA m^{-1}, while the temperature was kept at 25 °C. The magnetorheological properties were recorded by applying controlled shear rate mode 0.1—300 s^{-1}.

3. RESULTS AND DISCUSSION

3.1. Preparation

The preparation of polypyrrole/magnet-ite composites proceeds in two subsequent steps that follow in succession in the reaction mixture. At first, pyrrole is oxidized to a polypyrrole salt with iron(III) chloride that converts to iron(II) chloride, the stoichiometric oxidant-to-monomer mole ratio [$FeCl_3$]/[pyrrole] being 2.5 (Scheme S1). If the reaction mixture contains iron(III) ions in excess to the stoichiometric ratio, magnetite is produced in the second step after addition of ammonium hydroxide from the both iron chlorides.

When the oxidant-to-monomer mole ratio n = [$FeCl_3$]/ [pyrrole] exceeds the stoichiometric value, i.e., n > 2.5, then the oxidation of 1 mol of pyrrole with n mol of $FeCl_3$ yields 1 mol of polypyrrole constitutional units, and (n — 2.5) mol of $FeCl_3$ is left for the reaction with residual $FeCl_2$ after addition of ammonia to produce (n — 2.5)/2 mol of magnetite (**Scheme S1**). The predicted weight fraction of polypyrrole in the composite is

$$w_{\mathrm{ppy}} = \left(1 + \frac{n - 2.5}{2}\frac{M_{\mathrm{m}}}{M_{\mathrm{ppy}}}\right)^{-1} \qquad (1)$$

where M_m = 232 is the molecular weight of magnetite and MPPy = 63 is the molecular weight of the constitutional unit in the polypyrrole base (**Scheme 1**). For n = 2.5, only polypyrrole is produced (**Scheme S1**), while at n = 5 and 7.5 the content of polypyrrole in the composite was expected to be 17.9 and 9.8 wt %, respectively; that is, magnetite predominates in composites. For n > 7.5, the composition does not change anymore because iron(III) chloride has nothing the react with except possibly to cause the overoxidation of polypyrrole.

The above estimates just provide some guidance for the control of composite composition. The calculation, however, assumes that any residual iron(II) chloride stays dissolved in the ammonia solutions containing excess ammonia ions due to the formation of amo complexes and that it is removed by the subsequent washing of the composite, thus leaving a neat polypyrrole/magnetite composite. This condition need not be always satisfied due to the formation of partly soluble iron(II) oxide and hydroxide, and experimental compositions somewhat deviate from the prediction (**Figure 1**).

3.2. Yield

The relatively high yield of polypyrrole nanotubes per one gram of pyrrole, 1.6—1.7 g g^{-1} (**Table 1**), is due to the incorporation of protonating hydrochloric acid in the product (**Scheme 1**). The increase in the yield after the treatment with ammonia is due to the generation of iron oxides and hydroxides. At the mole ratio [$FeCl_3$]/[pyrrole] = 2.5, only iron(II) chloride should be present in the system. The high yield of composite could be still explained by the presence of poorly soluble iron(II) hydroxide. When increasing the concentration of $FeCl_3$, magnetite is produced (**Scheme S1**), and the yield increases accordingly.

3.3. Morphology

The nanotubular morphology of polypyrrole prepared at the stoichiometric ratio [$FeCl_3$]/ [pyrrole] = 2.5 in the presence of methyl orange (**Figure 2**, left) has been well established in the literature,6 and transmission electron microscopy confirms the presence of a cavity (Figure S1 in the **Supporting Information**). The diameter of nanotubes is 50—70 nm. Even when the oxidant concentration increased several times, the morphology and size of objects have not changed.

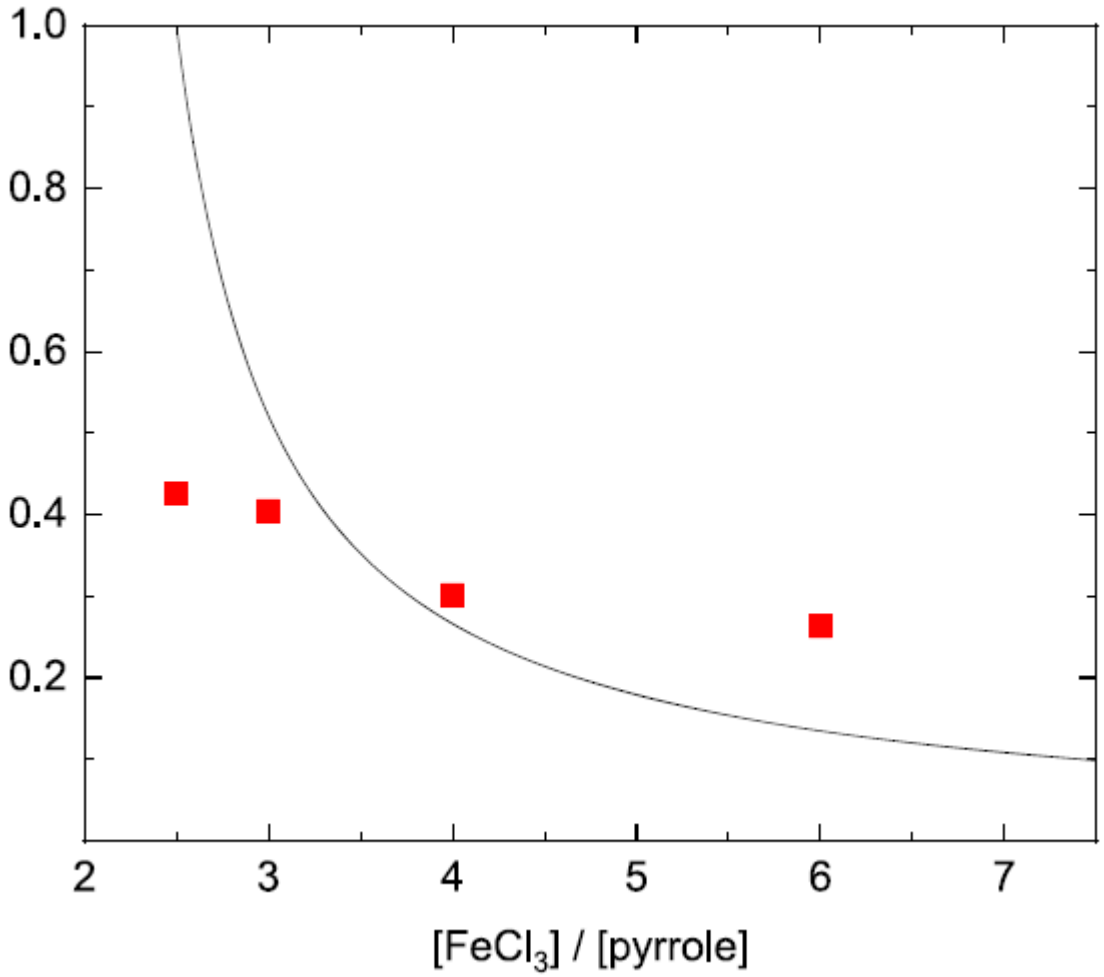

Figure 1. Calculated weight fraction of polypyrrole, WPPy, in the composite in dependence on mole ratio [FeCl3]/[pyrrole]. Experimental results are shown as squares.

Table 1. Yield of Polypyrrole Nanotubes and Polypyrrole/ Magnetite per Gram of Pyrrole and the Composite Composition before and after Reprotonation for Samples Prepared at Mole Ratio n = [$FeCl_3$]/[Pyrrole]

	yield, g g^{-1}		inorganic part, wt %	
n	PPy NT	PPy/magnetite	PPy/magnetite	reprotonated
2.5	1.61	4.16	57.3	32.4
3	1.64	4.70	59.6	19.9
4	1.66	6.00	69.9	14.6
6	1.72	8.76	73.7	48.3

Polypyrrole nanotubes are preserved after treatment with ammonia (**Figure 2**, right; **Figure S1**). At the stoichiometric ratio [$FeCl_3$]/[pyrrole] = 2.5, the oxidant should be consumed in the reaction with pyrrole (**Scheme S1**), and no magnetite was thus produced after adding ammonia solution. The microscopy, however, reveals and composition confirms (**Figure 1**) the presence of polydisperse inorganic particles. The magnetite particle prepared by the coprecipitation method were reported to

have a size of 10—40 nm,[30] and in the present case they had needle-like morphology with length 100—200 nm and cross section 30—50 nm (**Figure S1**). Polypyrrole nanotubes become also coated or decorated with magnetite (**Figure S1**), as confirmed below by FTIR spectroscopy. When increasing the ratio [$FeCl_3$]/[pyrrole], the amount of magnetite increases (the content of polypyrrole in **Figure 1** decreases), and nanotubes become incorporated in magnetite (**Figure 2**).

3.4. Composition

The increasing yield of solids with increasing concentration of iron(III) chloride is also confirmed by the determination of inorganic fraction in the composites as an ash (**Table 1**), which steadily increases (i.e., the content of polypyrrole decreases in **Figure 1**). After reprotonation of polypyrrole in 1 M hydrochloric acid, however, the content of inorganic fraction was substantially reduced. There are two reasons for the decrease in solids content after such treatment. The first is given by the fact that polypyrrole becomes reprotonated to the hydrochloride, and its relative participation becomes larger (**Scheme 1**). Magnetite is insoluble in acids, but this need not apply to magnetite nanoparticles. Also, other oxides or hydroxides that may accompany magnetite, such as iron(II) oxide, are partly soluble in hydrochloric acid. This is the second reason for the decrease in the content of iron oxides.

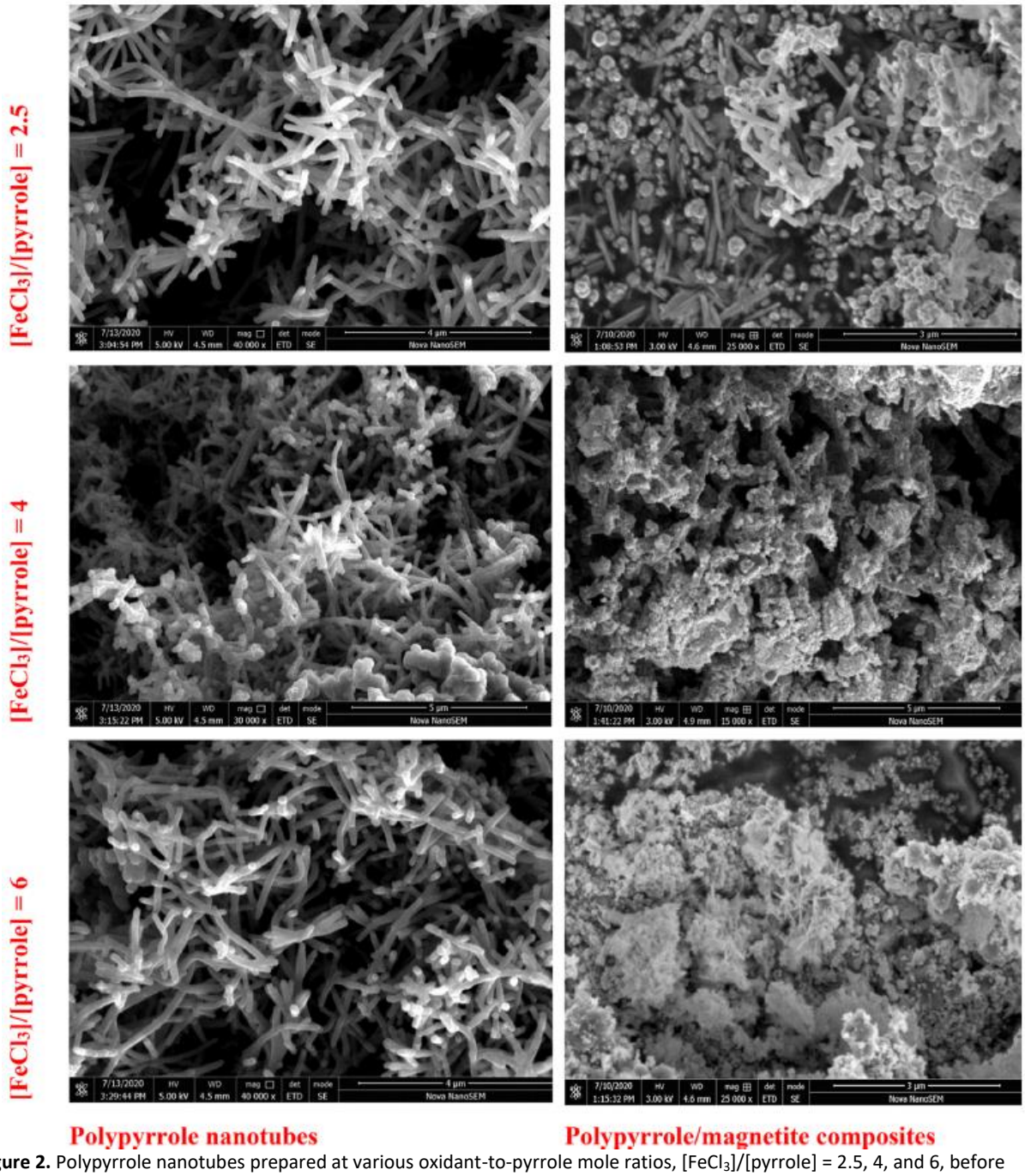

Figure 2. Polypyrrole nanotubes prepared at various oxidant-to-pyrrole mole ratios, [$FeCl_3$]/[pyrrole] = 2.5, 4, and 6, before (left) and after (right) the deposition of magnetite. Scale bars are 3-5 µm.

Table 2. Specific Surface Area and Volume of Pores for Samples Prepared at Mole Ratio n = [FeCy/[Pyrrole]

	specific surface area, $m^2\ g^{-1}$			volume of pores, $cm^3\ g^{-1}$		
n	polypyrrole nanotubes	polypyrrole/magnetite	reprotonated composite	polypyrrole nanotubes	polypyrrole/magnetite	reprotonated composite
2.5	82.4 ± 6.9	45.0 ± 1.4	40.4 ± 0.6	0.111 ± 0.007	0.172 ± 0.001	0.109 ± 0.001
6	54.2 ± 0.6	83.4 ± 0.5	58.1 ± 4.7	0.121 ± 0.014	0.227 ± 0.002	0.143 ± 0.006

3.5. Specific Surface Area

For some applications, such as magnetorheology,[41,42] which is going to be investigated later on, the specific surface area may be a parameter of interest. Just to remember, solid magnetic particles are dispersed in a nonmagnetic liquid, and the suspension viscosity can be increased by the applied magnetic field. The extent of solid-liquid interface is likely to affect the magnetorheological performance. The adsorbents of environmental pollutants,[43,44] such as organic dyes, based on conducting polymers and separable by magnetic field may also require enhanced specific surface area. For that reason, the specific surface area and pore volume are listed in **Table 2**. Adsorption/desorption isotherms are available in **Figure S2**.

The specific surface area of the globular polypyrrole reported in the literature was[3,4,5] 10.6 and 12.1 m^2 g^{-1}. For onedimensional polypyrrole morphologies this parameter was higher but still of the order of tens of m^2 g^{-1},[6,46,47] in accordance with the present results (**Table 2**). The specific surface area of magnetite alone is 21.4 ± 6.9 m^2 g^{-1}; its deposition onto polypyrrole nanotubes thus does not significantly affect this parameter of the polypyrrole/magnetite composite.

3.6. X-ray Diffraction

The resulting composites were studied by X-ray diffraction (Figure 3). Magnetite synthesized by the classical coprecipitation method was used as a reference.

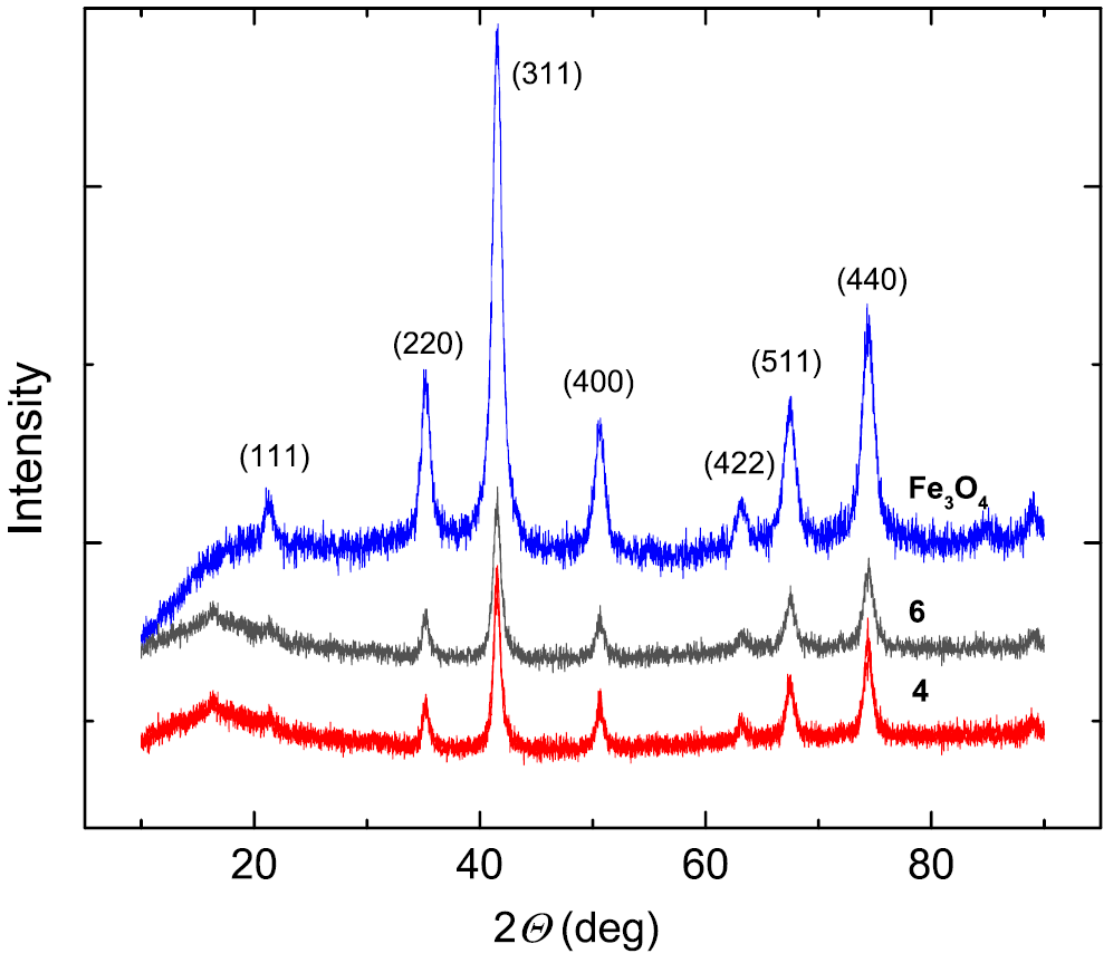

Figure 3. X-ray diffractograms of polypyrrole nanotubes/magnetite composites prepared at [$FeCl_3$]/[pyrrole] = 4 and 6 and the comparison with the magnetite prepared in the same manner in the absence of pyrrole.

X-ray diffraction patterns of samples and reference show peaks identified by crystallographic planes 111, 220, 311, 400, 422, 511, and 440, which correspond to magnetite. An alternative could only be maghemite which has an inverted spinel structure, showing peaks at very close positions. Noticeable amounts of other derivatives (oxides and hydroxides) of iron are not registered by diffraction patterns. The diffraction patterns of the composites in the range 10°-25° exhibit an amorphous halo associated with polypyrrole. Thus, the main components are polypyrrole and magnetite.

3.7. FTIR Spectroscopy

Infrared spectra reflect the molecular structure of neat polypyrrole nanotubes and in the composites with magnetite (**Figure 4**). In the first series (**Scheme 1**), when pyrrole was oxidized with iron(III) chloride, polypyrrole hydrochloride is produced.

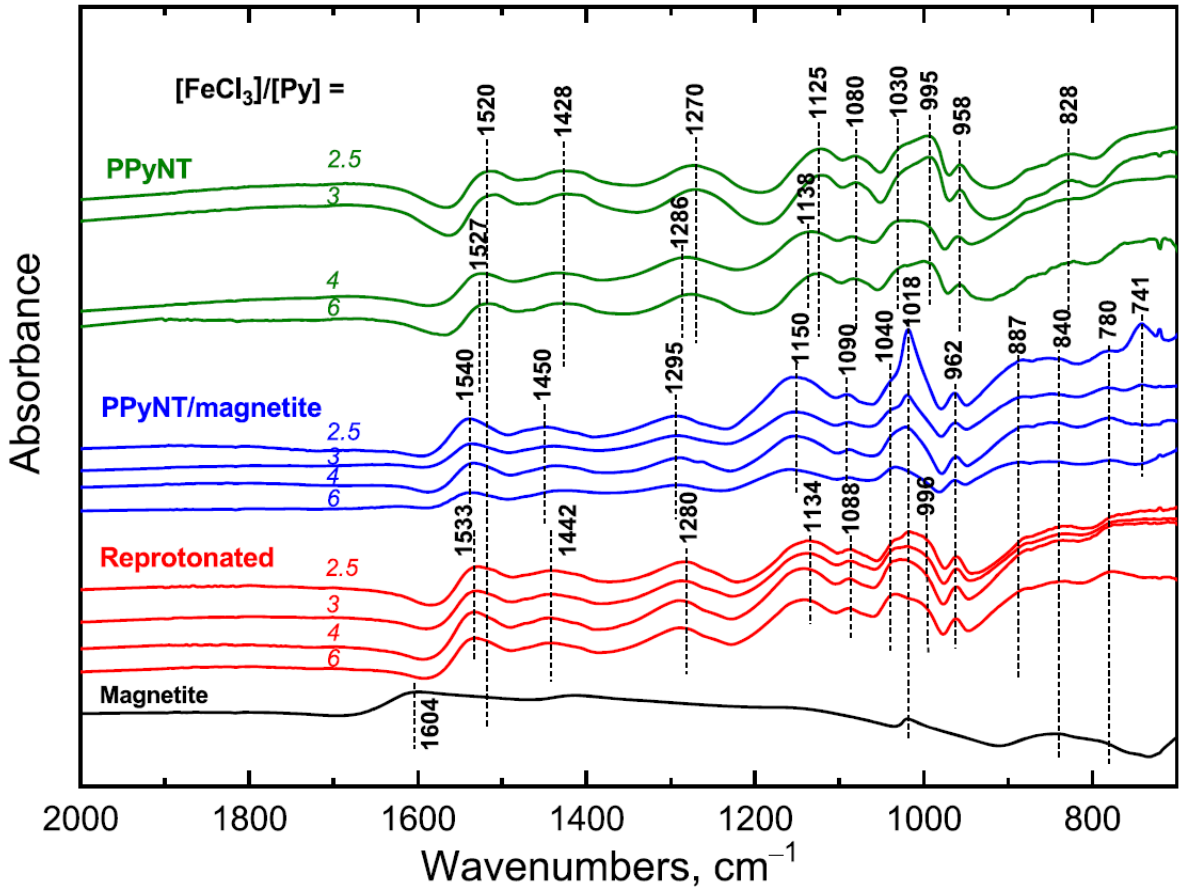

Figure 4. ATR FTIR spectra of polypyrrole nanotubes and their composite with magnetite before and after the reprotonation in dependence on the mole ratio [$FeCl_3$]/[pyrrole].

Close to the stoichiometric conditions, the infrared spectra of nanotubes (spectra 2.5 and 3 in polypyrrole nanotubes group in **Figure 4**) contain the main bands with maxima at 1520 cm^{-1} (C-C stretching vibrations in the pyrrole ring), 1428 cm^{-1} (C-N stretching vibrations in the ring), 1270 cm (C −H or C−N in-plane eformation modes), at 1125 and 1080 cm−1 (breathing vibrations of the pyrrole rings), at 1030 and 995 cm^{-1} (C−H and N−H in-plane deformation vibrations), and the peaks located at 958 and 828 cm^{-1} (C−H out-of-plane deformation vibrations of the ring).[6] When the concentration of oxidant increased to [$FeCl_3$]/[pyrrole] = 4 and 6, we observe the shifts of the main bands to 1527, 1286, and 1138 cm^{-1} and the relative increase of the ratio of the intensity of peaks situated at 1030 and 995 cm^{-1}, which corresponds to a slight deprotonation or overoxidation of polypyrrole.[8] This is reflected also in the decrease of the intensity of the broad band observed above 1800 cm^{-1}.

In the second series after treatment of samples with ammonia, magnetite is produced. Its presence is detected in the spectra (spectra 2.5, 3, and 4 in PPyNT/magnetite in **Figure 4**) by the peak situated at 1018 cm-1 which is observed in its spectrum (Magnetite in **Figure 4**) and also by enhancement of the intensity of a broad absorption band below 900 cm^{-1}. The maxima of the main bands of polypyrrole are shifted to 1540, 1450, 1295, and 1150 cm^{-1}, in agreement with the conversion of polypyrrole hydrochloride to a base8 (**Scheme 1**), which takes place under alkaline conditions. It correlates also with the lower conductivity of the composites observed below.

The suspension of composites in hydrochloric acid in the third series led to the reprotonation of polypyrrole which manifested itself by the shifts of the main bands to 1533, 1442, 1280, 1113, and 1088 cm^{-1} and by the reversed intensity ratio of peaks situated at 1030 and 996 cm^{-1}.[8] At the same time the peak of magnetite situated at 1018 cm^{-1} disappeared (spectra Reprotonated in **Figure 4**), which is connected with the partial dissolution of the iron oxides as discussed with respect to reaction yields above.

3.8. Conductivity

The conductivity of polypyrrole nanotubes, 22.7-25.1 S cm^{-1}, prepared at various [$FeCl_3$]/ [pyrrole] mole ratios is independent of this parameter within the experimental error (**Figure 5**), and they are not affected by the overoxidation suspected by FTIR spectra.

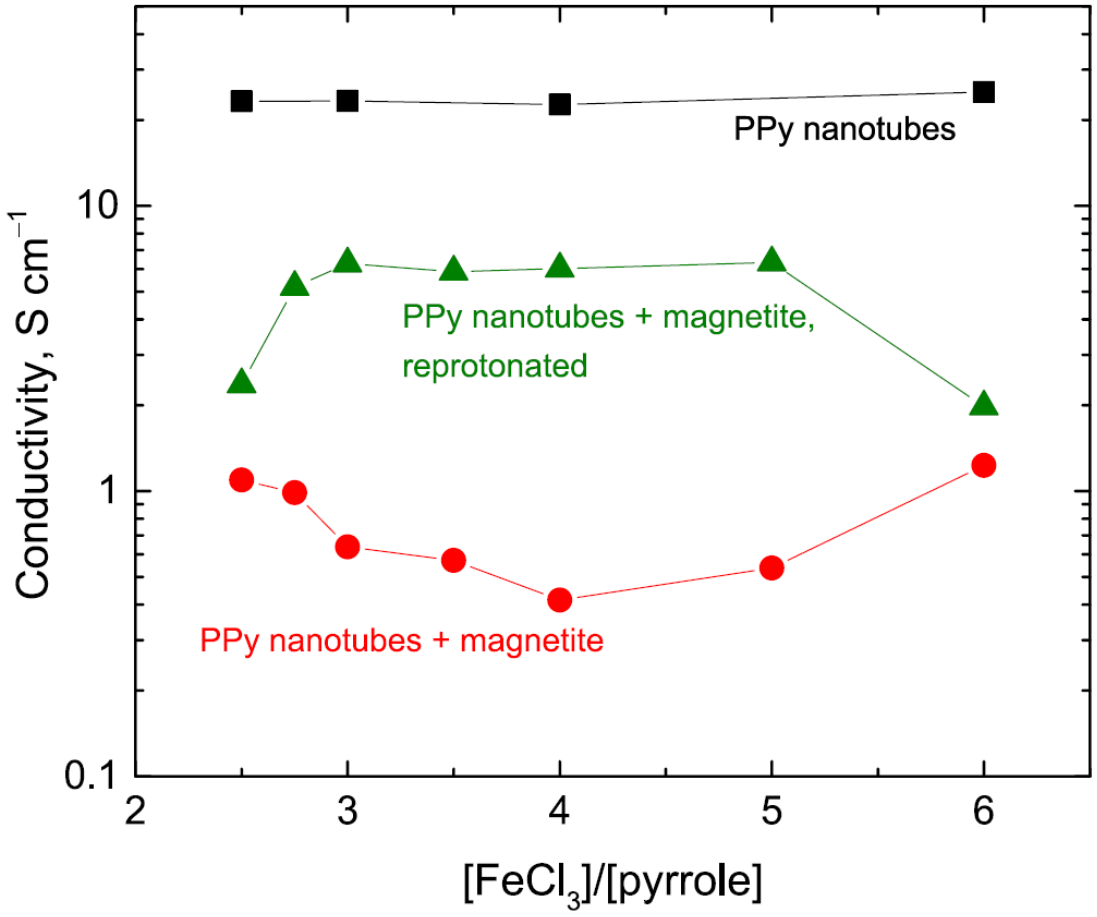

Figure 5. Conductivity of polypyrrole nanotubes (squares), polypyrrole nanotubes/magnetite (circles), and reprotonated composites (triangles) prepared at various [$FeCl_3$]/[pyrrole] mole ratios.

The conductivity of magnetite powder prepared by the coprecipitation method was lower than 10^{-3} S cm^{-1} and close to the value 1.3 X 10^{-3} S cm^{-1} reported in the literature.[30] For that reason the conductivity of polypyrrole/magnetite is reduced compared with neat nanotubes to the level close to 1 S cm^{-1} (**Figure 5**). It is again virtually independent of [$FeCl_3$]/[pyrrole] ratios, i.e., of the magnetite content in the composites (**Table 1**). Polypyrrole nanotubes obviously produce a percolating conducting network embedded within the magnetite matrix.

The reprotonation of polypyrrole in the composites with hydrochloric acid partially recovers the conductivity (**Figure 5**) as expected,[9] and as it is confirmed by FTIR spectra (**Figure 4**). The fact that a part of iron oxides dissolved and the fraction of polypyrrole increased (**Table 1**) also contributes do the conductivity recovery.

3.9. Magnetic Properties

Polypyrrole/magnetite composites display magnetic properties that are illustrated by the attraction to the permanent magnet (**Figure S3**). The magnetization curves for the individual composites are close to that of neat magnetite when [FeCl3]/[pyrrole] = 4 and 6 (Figure 6). For the [$FeCl_3$]/[pyrrole] = 2.5, the magnetic response is much weaker despite the nearly comparable content of inorganic part (**Table 1**). We can speculate that the inorganic component in latter case is based rather on iron(II) oxides or hydroxides than on magnetite, but the species are difficult to distinguish by X-ray diffraction or FTIR spectra.

The coercivity 28.4 Oe and the saturation magnetization 65 emu g^{-1} of magnetite prepared by the coprecipitation method were reported in the literature.[29] With increasing [$FeCl_3$]/[pyrrole] ratio, the saturation magnetization increased from 3 to 51 emu g^{-1} (**Figure 6**), which exceeds the saturation magnetization 35.6 emu g^{-1} at 60 wt % magnetite reported in the literature,[48] and the coercivity decreased from 112 to 12.6 Oe. The saturation magnetization of magnetite nanoparticles alone was 55 emu g^{-1}, i.e., lower than that of bulk magnetite, 92 emu g^{-1}.[48]

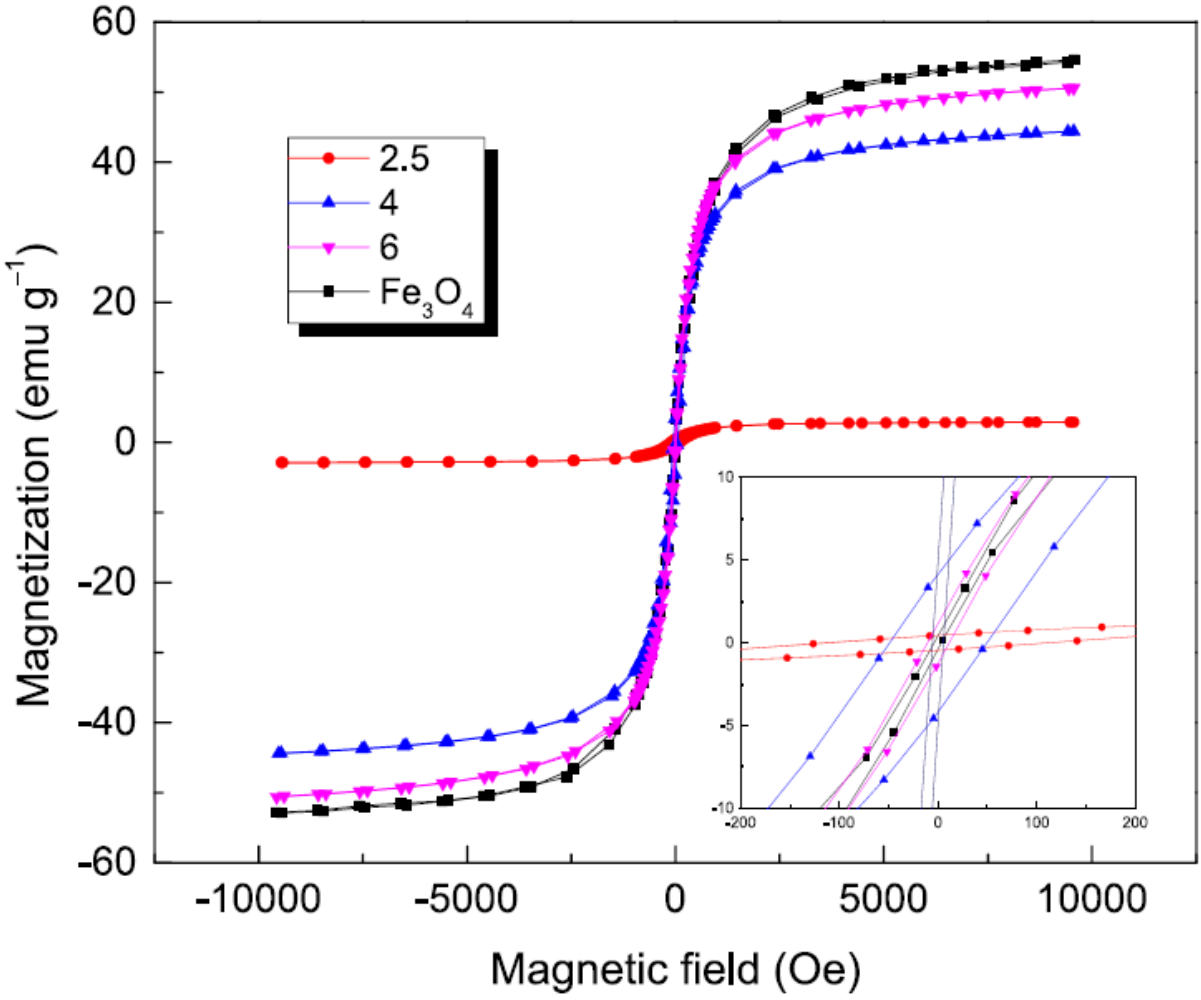

Figure 6. Magnetic properties of polypyrrole nanotubes/magnetite composites prepared at [$FeCl_3$]/[pyrrole] = 2.5, 4, and 6 and the comparison with magnetite prepared in the same manner in the absence of pyrrole. The inset illustrates the determination of coercivity.

Let us further compare the samples at the various stages of preparation. The polypyrrole nanotubes prepared with [$FeCl_3$]/[pyrrole] = 6 before ammonia treatment display the marginal saturation magnetization 0.1 emu g^{-1} and coercivity 323 Oe (**Figure 7**) probably due to the trace contamination of polypyrrole with iron compounds resulting from iron(III) chloride oxidant.

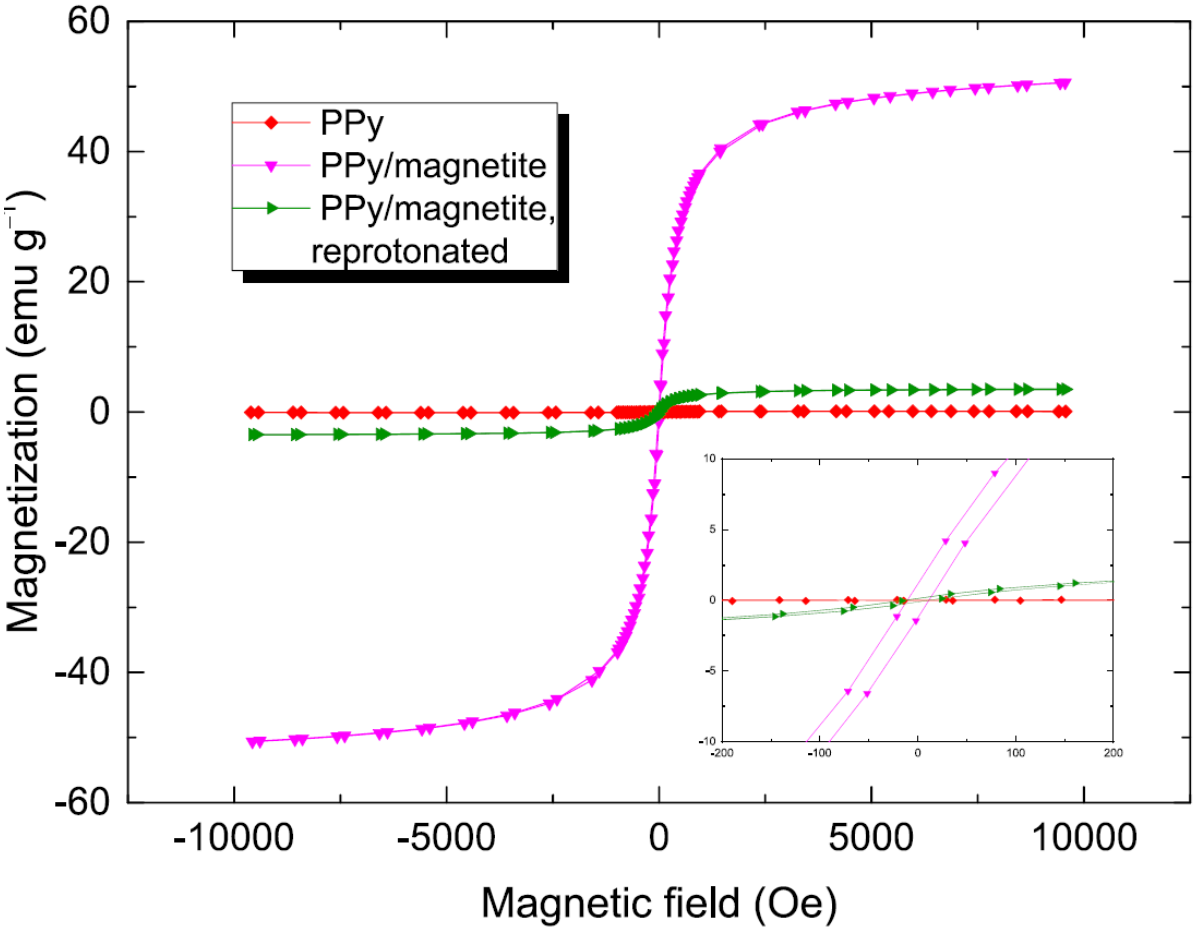

Figure 7. Magnetic properties of polypyrrole nanotubes, polypyrrole nanotubes/magnetite composite prepared at [$FeCl_3$]/[pyrrole] = 6, and the same composite after the reprotonation of polypyrrole.

After treatment with ammonia and consequent generation of magnetite, the saturation magnetization increased to 51 emu g^{-1} and the coercivity dropped to 12.6 Oe. The subsequent reprotonation of polypyrrole with hydrochloric acid reduced the saturation magnetization to 3.5 emu g^{-1}, the coercivity becoming 12.6 Oe as a result of the dissolution of some iron oxides, such as iron(II) oxide, accompanying magnetite. Magnetization thus was substantially reduced after the reprotonation of polypyrrole (**Figure 7**).

3.10. Magnetorheology

The rheological behavior of magnetorheological suspensions based on polypyrrole/magnet-ite composites prepared at [$FeCl_3$]/[pyrrole] = 4 and 6 in the absence as well as in the presence of an external magnetic field was performed to illustrate the possible use of suspensions in magnetic-field-responsive application. The systems exhibited typical behavior, and in the absence of the magnetic field, both suspensions behaved as pseudoplastic fluids, while a certain value of yield stress appeared after application of the external magnetic field as a consequence of developed aligned mesostructures of dispersed magnetized particles[49] (**Figure 8**). The flow curves in the on-state can be generally divided into two regions.

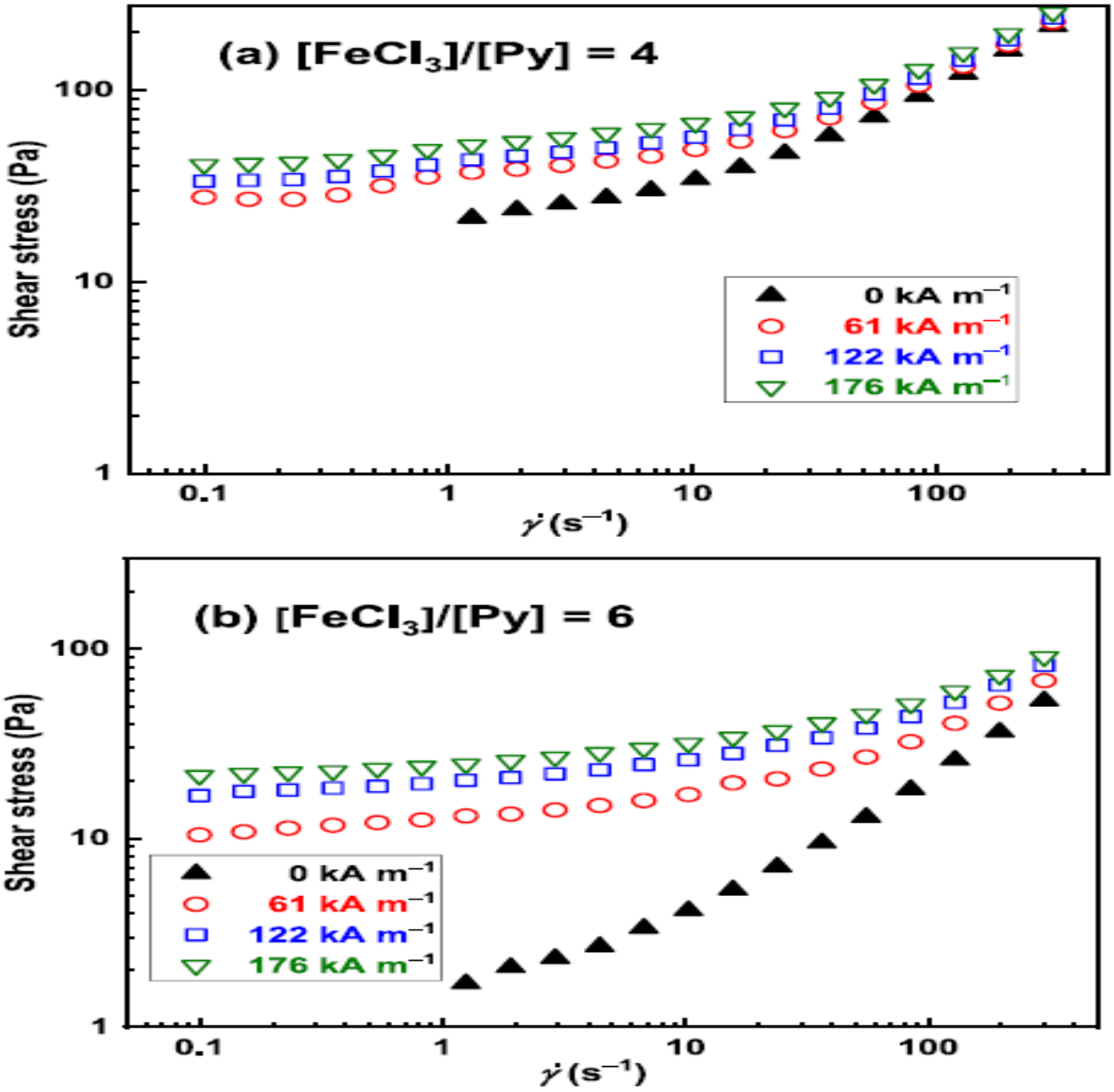

Figure 8. Double-logarithmic dependence of the shear stress on the shear rate for the prepared suspensions based on composite particles prepared at [$FeCl_3$]/[pyrrole] (a) 4 and (b) 6 at various magnetic field intensities.

The first is determined at the low-shear-rate region by the field-induced dipole interaction between dispersed particles, resulting in viscoplastic behavior. The second is determined at the high-shear-rate region by hydrodynamic forces, resulting in a standard flow character. In both cases, shear stresses were found to be higher for the system based on particles prepared at [$FeCl_3$]/[pyrrole] = 4 rate, due to their higher volume content in the suspension, leading to increased rotational diffusion.[50]

From the point of evaluation of magnetorheological performance, however, the difference between rheological parameters in the absence and in the presence of a magnetic field should be discussed. This increment is captured in **Figure 9**, which shows dependence of the ratio of T_M/T_0 on the shear rate, where τ_M and τ_0 stand for shear stress in the presence of a magnetic field and in its absence, respectively.

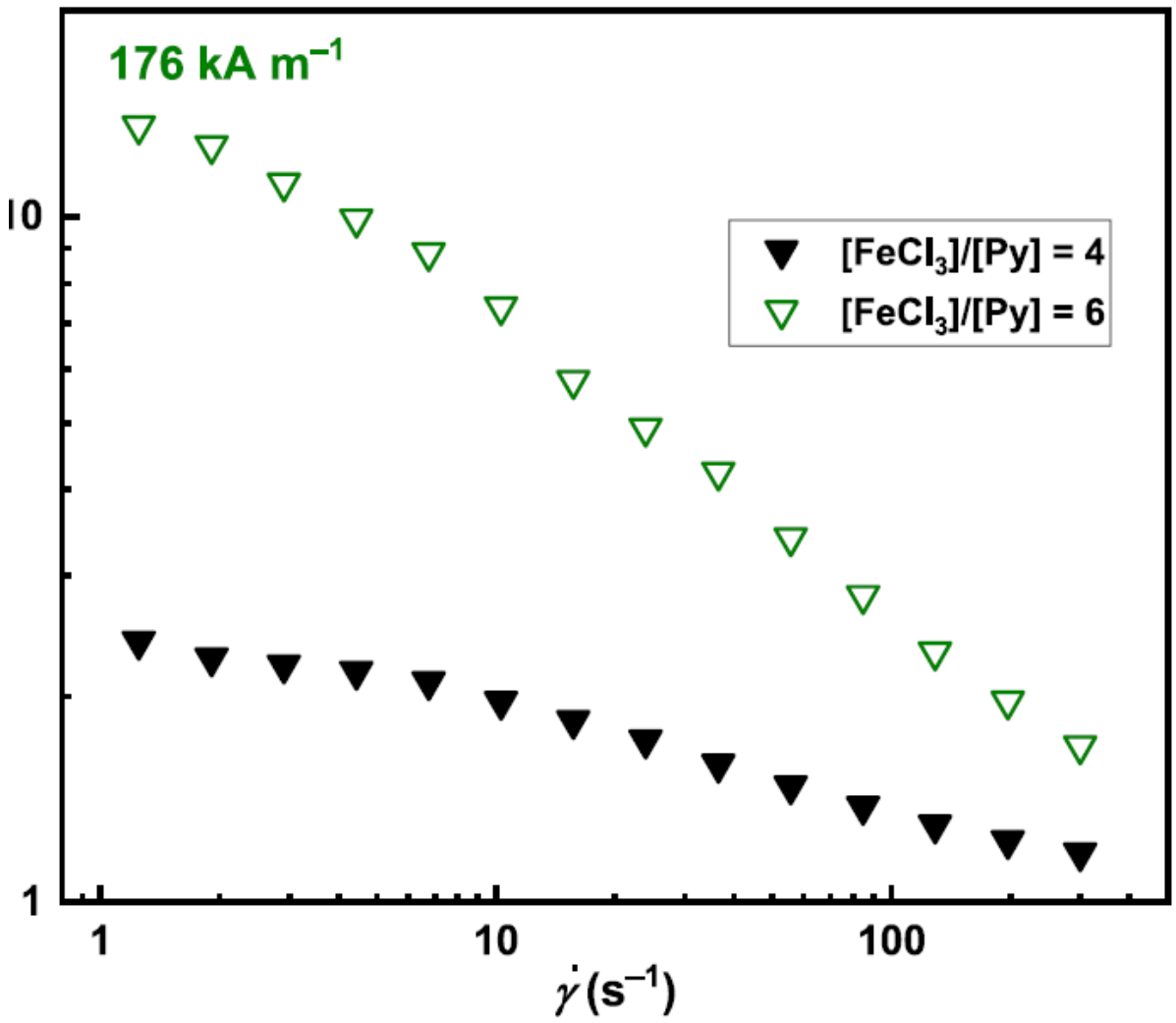

Figure 9. Efficiency of the prepared magnetorheological suspensions expressed as a ratio of shear stresses in the presence of a magnetic field (176 kA m^{-1}), T_M, and in its absence, T_0.

The highest ratio representing the highest increment in rheological parameters after application of the magnetic field was found for suspensions based on particles prepared at [$FeCl_3$]/ [pyrrole] = 6 due to their higher saturation magnetization. Nevertheless, both systems exhibit inferior magnetorheological performance due to lower saturation magnetization and lower loading of the particles. On the other hand, the particles have a high potential to be used as an additive in conventional magnetorheological suspensions in so-called bimodal systems due to their mild magnetic properties and morphology, which can increase overall performance of suspensions, such as enhanced sedimentation stability and redispersibility,[37,51,52] which will be further investigated. On the other hand, magnetorheological suspensions with similar effects as presented in this study can be used in various applications such as audio speakers where the high level of effect is not demanded.[53]

4. CONCLUSIONS

The study illustrates a simple way how to prepare conducting and magnetic composites of polypyrrole nanotubes and magnetite nanoparticles. Polypyrrole nanotubes are responsible for the enhanced conductivity of composites at the level of 1 S cm^{-1}, magnetite for magnetic ones. The one-pot preparation based on the oxidation of pyrrole with excess of iron(III) chloride takes place under

ambient conditions at room temperature, and it is completed in high yield within tens of minutes. The second step generates magnetite in the same reaction vessel after addition of ammonia followed.

One-dimensional morphology of particles is of importance in rheology of suspensions,[54] but the fact that the polypyrrole nanotubes are also conducting has not been exploited in this study. The conductivity, however, may provide an added value in specific applications. For example, the same systems can be used in magnetorhelogy and electrorheology[55] or in electromagnetic radiation shielding[32,35] when polypyrrole controls the reflection contribution, while magnetite supports the radiation absorption. In water-pollution treatment, polypyrrole is an efficient adsorbent of organic dyes,[43,44] and adsorption can be affected by applied electric potential, while magnetite allows for the separation of adsorbent by a magnetic field. The combination of magnetic and electrical properties is thus of potential benefit.

REFERENCES

(1) Stejskal, J. Conducting Polymers are not just Conducting: a Perspective for Emerging Technology. Polym. Int. 2020, 69, 662—664.

(2) Omastova, M.; Trchova, M.; Kovářova, J.; Stejskal, J. Synthesis and Structural Study of Polypyrroles Prepared in the Presence of Surfactants. Synth. Met. 2003, 138, 447—455.

(3) Li, Y.; Bober, P.; Trchova, M.; Stejskal, J. Polypyrrole Prepared in the Presence of Methyl Orange and Ethyl Orange: Nanotubes versus Globules in Conductivity Enhancement. J. Mater. Chem. C 2017, 5, 4236—4245.

(4) Stejskal, J.; Prokeš, J. Conductivity and Morphology of Polyaniline and Polypyrrole Prepared in the Presence of Organic Dyes. Synth. Met. 2020, 264, 116373.

(5) Sapurina, I.; Li, Y.; Alekseeva, E.; Bober, P.; Trchova, M.; Moravkova, Z.; Stejskal, J. Polypyrrole Nanotubes: the Tuning of Morphology and Conductivity. Polymer 2017, 113, 247—258.

(6) Stejskal, J.; Trchova, M. Conducting Polypyrrole Nanotubes: a Review. Chem. Pap. 2018, 72, 1563—1595.

(7) Minisy, I. M.; Acharya, U.; Kobera, L.; Trchova, M.; Unterweger, C.; Breitenbach, S.; Brus, J.; Pfleger, J.; Stejskal, J.; Bober, P. Highly Conducting 1-D Polypyrrole Prepared in the Presence of Safranin. J. Mater. Chem. C 2020, 8, 12140—12147.

(8) Stejskal, J.; Trchova, M.; Bober, P.; Moravkova, Z.; Kopecky, D.; Vmata, M.; Prokes, J.; Varga, M.; Watzlova, E. Polypyrrole Salts and Bases: Superior Conductivity of Nanotubes and their Stability towards the Loss of Conductivity by Deprotonation. RSC Adv. 2016, 6, 88382—88391.

(9) Prokes, J.; Varga, M.; Vrnata, M.; Valtera, S.; Stejskal, J.; Kopecky, D. Nanotubular Polypyrrole: Reversibility of Protonation/ Deprotonation Cycles and Long-Term Stability. Eur. Polym. J. 2019, 115, 290—297.

(10) HumpolíTek, P.; Kasparkova, V.; Pachermk, J.; Stejskal, J.; Bober, P.; Capakova, Z.; Radaszkiewicz, K. A.; Junkar, I.; Lehocky, M. The Biocompatibility of Polyaniline and Polypyrrole: A Comparative Study of their Cytotoxicity, Embryotoxicity and Impurity Profile. Mater. Sci. Eng., C 2018, 91, 303—310.

(11) Stejskal, J.; Sapurina, I.; Trchova, M.; Sedenkova, I.; Kovarova, J.; Kopecka, J.; Prokes, J. Coaxial Conducting Polymer Nanotubes: Polypyrrole Nanotubes Coated with Polyaniline or Poly(p-phenylenediamine) and Products of their Carbonization. Chem. Pap. 2015, 69, 1341 — 1349.

(12) Stejskal, J.; Trchova, M. Surfactants and Amino Acids in the Control of Nanotubular Morphology of Polypyrrole and their Effect on Conductivity. Colloid Polym. Sci. 2020, 298, 319—325.

(13) Jha, P.; Koiry, S. P.; Sridevi, C.; Putta, V.; Gupta, D.; Chauhan, A. K. A Strategy towards the Synthesis of Superhydrophobic/ Superoleophilic Non-Fluorinated Polypyrrole Nanotubes for Oil—Water Separation. RSC Adv. 2020, 10, 33747—33752.

(14) He, Q. M.; Rui, K.; Chen, C. H.; Yang, J. H.; Wen, Z. Y. Interconnected CoFe2O4—Polypyrrole Nanotubes as Anode Materials for High Performance Sodium Ion Batteries. ACS Appl. Mater. Interfaces 2017, 9, 36927—3695.

(15) Zou, Y. H.; Wang, H. N.; Sun, H. X.; Lin, Z. X.; Wang, F.; Zhang, X.; Wang, L. J.; Meng, X.; Zhou, Z. Y. Construction of Polypyrrole Nanotubes Interconnected ZIFs-Templated Nickel-Cobalt Layered Double Hydroxide via Varying the Mass of ZIF-67 for Supercapacitors with Tunable Performance. Mater. Chem. Phys. 2020, 255, 123497.

(16) Ji, J. Y.; Zhang, X. Y.; Liu, J.; Peng, L. F.; Chen, C. L.; Huang, Z. L. ; Li, L.; Yu, X. H.; Shang, S. M. Assembly of Polypyrrole Nanotube@MnO2 Composites with an Improved Electrochemical Capacitance. Mater. Sci. EngB 2015, 198, 51-56.

(17) Yuan, H. R; Deng, L. F.; Tang, J. H.; Zhou, S. G.; Chen, Y.; Yuan, Y. Facile Synthesis of MnO2/Polypyrrole/MnO2 Multiwalled Nanotubes as Advanced Electrocatalysts for the Oxygen Reduction Reaction. ChemElectroChem. 2015, 2, 1152-1158.

(18) Zhang, D. X.; Zhang, Z.; Xu, X. J.; Zhang, Q.; Yuan, C. W. Flexible MoS2 Nanosheets/Polypyrrole Nanofibers for Highly Efficient Electrochemical Hydrogen Evolution. Phys. Lett. A 2017, 381, 3584-3588.

(19) Wolfart, F.; Dubal, D. P.; Vidotti, M.; Gomez-Romero, P. Hybrid Core-Shell Nanostructured Electrodes Made of Polypyrrole Nanotubes Coated with Ni(OH)2 Nanoflakes for High-Energy-Density Supercapacitors. RSC Adv. 2016, 6, 15062-15070.

(20) Yue, J.; Wang, W. P.; Wang, N. N.; Yang, X. F.; Feng, J. K.; Yang, J.; Qian, Y. T. Triple-Walled SnO2@N-Doped Carbon-SnO2 as an Advanced Anode Material for Lithium and Sodium Storage. J. Mater. Chem. A 2015, 3, 23194-23200.

(21) Du, X. F.; Yang, T. J.; Lin, J.; Feng, T. Y.; Zhu, J. B.; Lu, L.; Xu, Y. L.; Wang, J. P. Microwave-Assisted Synthesis of SnO2@Polypyrrole Nanotubes and their Pyrolized Composite as Anode for Lithium-Ion Batteries. ACS Appl. Mater. Interfaces 2016, 8, 15598-15606.

(22) Kaur, A.; Kumar, R. Sensing of Ammonia at Room Temperature by Polypyrrole-Tin Oxide Nanostructures: Investigation by Kelvin Probe Force Microscopy. Sens. ActuatorsA 2016, 245, 113-118.

(23) Ruan, B.; Guo, H.; Liu, Q.; Shi, D.; Chou, S.; Liu, H.; Chen, G.; Wang, J. 3D Structured SnO2-Polypyrrole Nanotubes Applied in Na-Ion Batteries. RSC Adv. 2016, 6, 103124-103131.

(24) Cao, Z. Z.; Yang, H. Y.; Dou, P.; Wang, C.; Zheng, J.; Xu, X. H. Synthesis of Three-Dimensional Hollow SnO2@PPy Nanotube Array via Template-Assisted Method and Chemical Vapor-Phase Polymerization as High Performance for Lithium-Ion Batteries. Electrochim. Acta 2016, 209, 700-708.

(25) Stejskal, J. Conducting Polymer-Silver Composites. Chem. Pap. 2013, 67, 814-848.

(26) Sapurina, I.; Stejskal, J.; Sedenkova, I.; Trchova, M.; Kovařova, J.; Hromadkova, J.; Kopecká;, J.; Cieslar, M.; Abu El-Nasr, A.; Ayad, M. M. Catalytic Activity of Polypyrrole Nanotubes Decorated with Noble-Metal Nanoparticles and their Conversion to Carbonized Analogues. Synth. Met. 2016, 214, 14-22.

(27) Pei, F. B.; Wang, P.; Ma, E. H.; Yu, H. X.; Gao, C. X.; Yin, H. B.; Li, Y. Y.; Liu, Q.; Dong, Y. H. A Sandwich-Type Amperometric Immunosensor Fabricated by Au@Pd NDs/Fe2+-CS/PPyNTs and Au NPs/NH2-GS to Detect CEA Sensitively via Two Detection Methods. Biosens. Bioelectron. 2018, 122, 231-238.

(28) Zhang, X. J.; Sheng, Q. L.; Zheng, J. B. Synthesis of Palladium Nanocubes Decorated Polypyrrole Nanotubes and its Application for Electrochemical Sensing. J. Iran. Chem. Soc. 2019, 16, 1061-1069.

(29) Qiu, G. H.; Wang, Q.; Nie, M. Polypyrrole-Fe3O4 Magnetic Nanocomposite Prepared by Ultrasonic Irradiation. Macromol Mater. Eng. 2006, 291, 68-74.

(30) Petcharoen, K.; Sirivat, A. Synthesis and Characterization of Magnetite Nanoparticles via the Chemical Co-Precipitation Method. Mater. Sci. Eng.. B 2012, 177, 421-427.

(31) Getiren, B.; Ciplak, Z.; Gokalp, C.; Yildiz, N. NIR-Responsive Fe3O4@PPy Nanocomposite for Efficient Potential Use in Photothermal Therapy. J. Appl. Polym. Sci. 2020, 137, 49343.

(32) Liu, F. B.; Li, C. P.; Jiang, X. H.; Waterhouse, G. I. N.; Xing, C. J.; Zhang, Z. M.; Yu, L. M. Novel Three-Dimensional TiO2-Fe3O4@ Polypyrrole Composites with Tunable Microwave Absorption in the 2-40 GHz Frequency Range. J. Mater. Sci. 2020, 55, 15493-15509.

(33) Goswami, B.; Mahanta, D. Polyaniline-Fe3O4 and Polypyrrole-Fe3O4 Magnetic Nanocomposites for Removal of 2,4-Dichlorophe-noxyacetic Acid from Aqueous Medium. J. Environ. Chem. Eng. 2020, 8, 103919.

(34) Tang, S.; Lan, Q.; Liang, J.; Chen, S.; Liu, C.; Zhao, J.; Cheng, Q.; Cao, Y.-C.; Liu, J. Facile Synthesis of Fe3O4@PPy Core-Shell Magnetic Nanoparticles and their Enhanced Dispersity and Acid Stability. Mater. Des. 2017, 121, 47-50.

(35) Chen, X. L.; Shi, T.; Wu, G. L.; Lu, Y. Design of Molybdenum Disulfide@Polypyrrole Composite Decorated with Fe3O4 and Superior Electromagnetic Wave Absorption Performance. J. Colloid Interface Sci. 2020, 572, 227-235.

(36) Ma, G. Q.; Wen, Z. Y.; Wang, Q. S.; Shen, C.; Peng, P.; Jin, J.; Wu, X. W. Enhanced Performance of Lithium Sulfur Battery with SelfAssembly Polypyrrole Nanotube Film as the Functional Interlayer. J. Power Sources 2015, 273, 511-516.

(37) Plachy, T.; Cvek, M.; KoZakova, Z.; Sedlaak, M.; Moučka, R The Enhanced MR Performance of Dimorphic MR Suspensions Containing either Magnetic Rods or their Non-Magnetic Analogs. Smart Mater. Struct. 2017, 26, 025026.

(38) Yoon, D. S.; Kim, G. W.; Choi, S. B. Response Time of Magnetorheological Dampers to Current Inputs in a Semi-Active Suspension System: Modeling, Control and Sensitivity Analysis. Mech. Syst. Signal Process. 2021, 146, 106999.

(39) Chen, D. P.; Song, A. G.; Tian, L.; Ouyang, Q. Q.; Xiong, P. W. Development of a Multidirectional Controlled Small-Scale Spherical MR Actuator for Haptic Applications. IEEE/ASME Trans. Mechatron. 2019, 24, 1597.

(40) Xia, Z. B.; Fang, F. Z.; Ahearne, E.; Tao, M. R. Advances in Polishing of Optical Freeform Surfaces: A Review. J. Mater. Process. Technol 2020, 286, 116828.

(41) Kim, J. H.; Fang, F. F.; Choi, H. J.; Seo, Y. Magnetic Composites of Conducting Polyaniline/Nano-Sized Magnetite and their Magnetorheology. Mater. Lett. 2008, 62, 2897-2899.

(42) Dong, Y. Z.; Choi, K.; Kwon, S. H.; Nam, J. D.; Choi, H. J. Nanoparticles Functionalized by Conducting Polymers and their Electrorheological and Magnetorheological Applications. Polymers 2020, 12, 204.

(43) Stejskal, J. Interaction of Conducting Polymers, Polyaniline and Polypyrrole, with Organic Dyes: Polymer Morphology Control, Dye Adsorption and Photocatalytic Decomposition. Chem. Pap. 2020, 74, 1 - 54.

(44) Sapurina, I. Yu.; Shishov, M. A.; Ivanova, V. T. Sorbents for Water Purification based on Conjugated Polymers. Russ. Chem. Rev. 2020, 89, 1115-1131.

(45) Wang, Z.; Goyal, N.; Liu, L. Y.; Tsang, D. C. W.; Shang, J.; Liu, W. J.; Li, G. N-Doped Porous Carbon Derived from Polypyrrole for CO2 Capture from Humid Flue Gases. Chem. Eng. J. 2020, 396, 125376.

(46) Kopecka, J.; Kopecky, D.; Vmata, M.; Fitl, P.; Stejskal, J.; Trchova, M.; Bober, P.; Momvkova, Z.; Prokes, J.; Sapurina, I. Polypyrrole Nanotubes: Mechanism of Formation. RSC Adv. 2014, 4, 1551-1558.

(47) Kopecky, D.; Varga, M.; Prokes, J.; Vmata, M.; Trchova, M.; Kopecka, J.; Vaclavík, M. Optimization Routes for High Electrical Conductivity of Polypyrrole Nanotubes Prepared in the Presence of Methyl Orange. Synth. Met. 2017, 230, 89-96.

(48) Yamaura, M; Camilo, R.L; Sampaio, L.C; Macedo, M.A; Nakamura, M; Toma, H.E. Preparation and Characterization of (3-Aminopropyl) Triethoxysilane-Coated Magnetite Nanoparticles. J. Magn. Magn. Mater. 2004, 279, 210-217.

(49) Choi, H. J.; Zhang, W. L.; Kim, S.; Seo, Y. Core-Shell Structured Electro- and Magneto-Responsive Materials: Fabrication and Characteristics. Materials 2014, 7, 7460-7471.

(50) Rodriguez-Arco, L.; Lopez-Lopez, M. T.; Kuzhir, P.; Gonzalez-Caballero, F. How Nonmagnetic Particles Intensify Rotational Diffusion in Magnetorheological Fluids. Phys. Rev. E 2014, 90, 012310.

(51) Sedlacík, M.; Pavlínek, V.; Vyroubal, R.; Peer, P.; Filip, P. A Dimorphic Magnetorheological Fluid with Improved Oxidation and Chemical Stability under Oscillatory Shear. Smart Mater. Struct. 2013, 22, 035011.

(52) Morillas, J. R.; Bombard, A. J. F.; de Vicente, J. Magnetorheology of Bimodal Fluids in the Single-Multidomain Limit. Ind. Eng. Chem. Res. 2018, 57, 13427-13436.

(53) Purnomo, E. D.; Ubaidillah, U.; Imaduddin, F.; Yahya, I.; Mazlan, S. A. Preliminary Experimental Evaluation of a Novel Loudspeaker Featuring Magnetorheological Fluid Surround Absorber. Indones. J. Electr. Eng. Comput. Sci 2020, 17, 922-928.

(54) Lee, J. Y.; Kwon, S. H.; Choi, H. J. Magnetorheological Characteristics of Carbonyl Iron Microparticles with Different Shapes. Korea-Australia Rheol J. 2019, 31, 41-47.

(55) Park, D. E.; Chae, H. S.; Choi, H. J.; Maity, A. Magnetite-Polypyrrole Core-Shell Structured Microspheres and their Dual Stimuli-Response under Electric and Magnetic Fields. J. Mater. Chem. C 2015, 3, 3150-3158.